Journal of Sensor Science and Technology
Vol. 30, No. 4 (2021) pp. 218-222
http://dx.doi.org/10.46670/JSST.2021.30.4.218
pISSN 1225-5475/eISSN 2093-7563

Designing a nanocrystal-based temperature and strain multi-sensor with one-step inkjet printing

Junsung Bang[1], Junhyuk Ahn[1], and Soong Ju Oh[1,+]

Abstract

Wearable multi-sensors based on nanocrystals have attracted significant attention, and studies on patterning technology to implement such multi-sensors are underway. Conventional patterning processes may affect material properties based on high temperatures and harsh chemical conditions. In this study, we developed an inkjet printing technique that can overcome these drawbacks through the application of patterning processes at room temperature and atmospheric pressure. Nanocrystal-based ink is used to adjust properties efficiently. Additionally, the viscosity and surface tension of the solvents are investigated and optimized to increase patterning performance. In the patterning process, the electrical, electrothermal, and electromechanical properties of the nanocrystal pattern are controlled by the ligand exchange process. Experimental results demonstrate that a multi-sensor with a temperature coefficient of resistance of 3.82×10^{-3} K^{-1} and gauge factor of 30.6 can be successfully fabricated using one-step inkjet printing.

Keywords : Nanocrystal, Inkjet printing, One-step, Surface chemistry, Ligand exchange, Multi-sensor.

1. INTRODUCTION

The development of various electronic devices [1,2], such as wearable multi-sensors [3–8], based on nanoparticles is well underway. Accordingly, circuit patterning technology is in high demand to facilitate the development of various multi-sensors. Modern patterning techniques include a photolithography process using photoresist materials and a thermal deposition process. However, these methods are complex and require expensive equipment. In this study, to overcome the disadvantages of the patterning processes mentioned above, a one-step patterning process using inkjet printing was developed.

In inkjet printing, the process of printing patterns on substrates using colloidal nanocrystal (NC) ink is not only mask-free, on-demand, and requiring no contact with materials, but it is also cheap and fast advantages because this process involves directly converting digital images into substrates. Additionally, NCs can be used as ink because they are surrounded by organic shells (ligands) that are easily dispersed in non-polar solvents. Furthermore, NCs have been applied to various temperature, strain, and pressure wearable sensors [9–13] because their properties can be adjusted by controlling the surface ligand exchange process based on their large surface-to-volume ratio.

In this work, based the characteristics described above, NC colloidal ink was printed and patterned directly on a substrate to fabricate multi-sensor arrays. Subsequently, a ligand exchange process was conducted to adjust the electrical, electrothermal, and electromechanical properties of the fabricated NC patterns, as well as the inter-particle distances between NCs. Therefore, the conduction mechanisms [14] of NC thin films can be controlled by the ligand exchange process. In this manner, temperature and strain sensors can be fabricated. In this study 300 μm linewidth sensor patterns were successfully developed using inkjet printing, demonstrating that this technology can contribute to the manufacturing of next-generation devices, such as smart wearable healthcare systems.

2. EXPERIMENTAL SETUP

2.1 Materials

Oleic acid (OA, 90%), oleylamine (OAm, 70%), tetrabutylammonium bromide (TBAB, ≥99%), toluene (99.8%), ethanol (≥99.5%), octane (99+%), isopropanol (99.5%), and (3-

[1] Department of Materials Science and Engineering, Korea University
145, Anam-ro Seongbuk-gu, Seoul 02841, Republic of Korea
[+]Corresponding author: sjoh1982@korea.ac.kr
(Received: Jul. 12, 2021, Revised: Jul. 28, 2021, Accepted: Jul. 29, 2021)

mercaptopropyl) trimethoxysilane (MPTS, 95%) were obtained from Sigma-Aldrich, Co. Silver nitrate ($AgNO_3$, 99.9+%) was purchased from Alfa Aeser, Co. Cyclohexylbenzene (98%) was obtained from Acros Organics, Co. All reagents were used without further purification.

2.2 Silver nanocrystal synthesis

Silver NCs were synthesized following the methods of previous studies reported in the literature with minor modifications. $AgNO_3$ (0.68 g), OAm (2.0 mL), and OA (18.0 mL) were combined in a 100 mL three-neck flask. The mixture was degassed at 70 °C for 1 h. After degassing, the three-neck flask was filled with nitrogen gas and heated to 180 °C at a rate of 1 °C/min. After the temperature reached 180 °C, the reaction was stopped and the mixture solution was cooled in air to room temperature. After synthesis, the mixture solution was washed using ethanol and toluene. In this work, the washed silver NCs were redispersed in cyclohexylbenzene (CHB) and octane solvents with a concentration of 100 mg mL^{-1}.

2.3 Characterization

An inkjet printer (FUJIFILM, Dimatix Materials PrinterDMP-2831) was used to pattern Ag NCs. X-ray diffraction spectroscopy (D/MAX-2500 V, Rigaku) was used to confirm the ligand exchange process. Ultraviolet–visible (UV–vis) spectroscopy (Cary 5000, Agilent Technologies) and Fourier transform infrared (FTIR) spectroscopy (LabRam ARAMIS IR2) were used to characterize optical and chemical properties. A probe station (MST-4000A, MSTECH) was used to measure electrical conductivity.

3. RESULTS AND DISCUSSION

3.1 Engineering overview and inkjet printing strategy

In this study, silver NC thin film patterns were deposited on a substrate using an inkjet printing process and the properties of the thin films were adjusted through the ligand exchange process (Fig. 1(a)). The most important aspect of fabricating thin films via inkjet printing is the adjustment of the viscosity and surface tension of the ink, as well as the adhesion with the substrate. If the viscosity and surface tension of the ink are inappropriate, inkjet printing will not be possible, necessitating a more complex

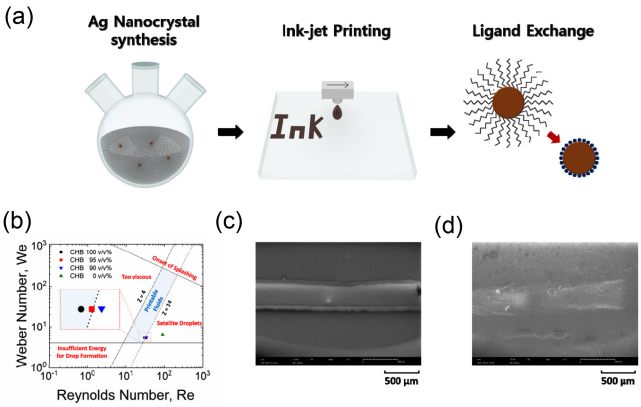

Fig. 1. (a) Scheme for silver NC synthesis, inkjet printing, and ligand exchange process, (b) Re-We plot for confirming the Z value, (c), (d) Scanning electron microscopy (SEM) images of CHB 95 v/v% silver NC patterns with MPTS treatment and without MPTS treatment, respectively.

patterning process. Furthermore, if the adhesion between the thin film and ink is not sufficient, problems such as lift-off can occur during the ligand exchange process following the patterning process.

Silver NCs with a size of 4 nm were synthesized using OA and OAm as surface ligands n a wet chemical method. Therefore, the surfaces of the NCs were surrounded by long organic ligands. This makes the NCs suitable for inkjet printing based on their high stability. However, dispersion in a commonly used octane solvent is inappropriate for inkjet printing based on the low viscosity of such solvents. To achieve proper control of the viscosity and surface tension of the ink, we added CHB to the silver NC ink, which has a relatively high viscosity. In this study, an Re-We plot was used to identify solvents with appropriate levels of viscosity and surface tension with Z values between 4 and 14. As a result, we determined that inkjet printing is possible under conditions with CHB > 95 v/v% (Fig. 1(b)). We adopted a 95 v/v% solvent rather than a CHB 100 v/v% solvent because incorporating an octane solvent can reduce the coffee ring effect. Using inkjet printing with the conditions defined above, silver NC thin film patterns with a 300 μm line width were successfully deposited. Fig. 1(c) presents an SEM image of a deposited film. Next, we introduced the self-assembled monolayer (SAM) formation method to improve adhesion between the substrates and thin films. The SAM formation steps are as follows. 1) Conduct UV-ozone treatment above the glass substrate to form -OH on the surface. 2) Immerse the surface of the glass in an MPTS solution for more than 12 h to exchange -OH with -SH, which improves the adhesion between the silver NCs and substrate. A non-MPTS-

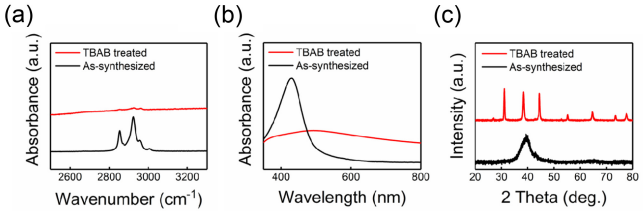

Fig. 2. As-synthesized TBAB-ligand-treated silver NC thin films: (a) FTIR data, (b) UV–vis data, and (c) X-ray diffraction (XRD) data.

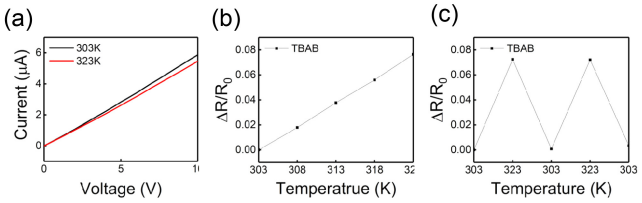

Fig. 3. Temperature sensors with TBAB-treated silver NC thin films. (a) Electrical properties at 303 K and 323 K, (b) Resistance-temperature curve measured at 5 K intervals between 303 K and 323 K under 10 V, (c) Cycle testing data from 303 K to 323 K under 10 V.

treated substrate cannot form normal patterns, as shown in (Fig. 1(d)). Based on the two strategies defined above, we developed a direct patterning technique.

3.2 Chemical, optical, and structural analysis

In this study, we developed a temperature and strain sensor by applying ligand treatment to silver NC thin film patterns formed through inkjet printing to adjust their electrical, electrothermal, and electromechanical characteristics. The temperature and strain sensors that we developed are resistive-type sensors that measure temperature and strain by analyzing changes in conductivity (changes in resistance) caused by changes in temperature and strain. The silver nanoparticles used in the fabrication of temperature and strain sensors are surrounded by long organic ligands, such as OA and OAm, and these long organic ligands do not exhibit electrical properties based on the large distances between particles. In this study, the TBAB ligand [15–16] was used to adjust conduction properties and silver NCs were used as the active layers of the sensor. Accordingly, after synthesizing 4 nm silver NCs, chemical, optical, and structural analysis was performed to confirm ligand exchange (Fig. 2).

First, FTIR spectroscopy of the as-synthesized and TBAB-treated silver NC thin films on a glass substrate was conducted (Fig. 2(a)). In the case of the as-synthesized silver NCs, CH bonds were present in OA and OAm, resulting in a peak at approximately 2900 cm^{-1}. In contrast, the TBAB-treated silver NCs exhibited no peak around 2900 cm^{-1}. This indicates that ligand exchange occurred.

Similarly, the UV–vis spectroscopy results contained a peak at 432 nm for the as-synthesized silver NCs. By applying the Scherrer equation to these results, we determined that 4 nm silver NCs were successfully synthesized. The UV–vis results of the TBAB-ligand-treated silver NC thin films exhibited a broad localized surface plasmon resistance peak at approximately 432 nm, which is a result of sintering during the ligand exchange process. This is because during the process of TBAB treatment, the long organic ligands are transformed into short TBAB ligands and physical contact between the silver NCs occurs, resulting in sintering. The differences between the as-synthesized and TBAB-treated data confirm that ligand exchange occurred.

Finally, XRD spectroscopy revealed a diffraction peak at $2\theta = 39.1°$ corresponding to the {111} plane for the as-synthesized silver NCs. The TBAB-treated silver NCs exhibited strong diffraction peaks at $2\theta = 31.3°$, 44.6°, and 38.2°, corresponding to the {200} and {220} planes of AgBr and {111} plane of Ag, respectively. This implies that ligand exchange and sintering were successfully occurred. After sintering, the average size of 32.84 nm for the TBAB-treated Ag NCs was calculated by using Scherrer's equation. Therefore, our chemical, optical, and structural analyses confirmed that 4 nm silver NCs were synthesized and that the TBAB ligand exchange process successfully occurred.

3.3 Demonstration of a multi-sensor

The electrical and electrothermal properties of the TBAB-ligand-treated silver NC thin film patterned temperature sensors fabricated through inkjet printing were investigated. The performance of the fabricated temperature sensors can be determined based on the temperature-resistance coefficient (TCR), which can be expressed as

$$TCR = (\Delta R/R_0)/\Delta T, \quad (1)$$

where ΔR, R_0, and ΔT are the resistance change, initial resistance, and temperature change, respectively.

First, the electrical properties of the TBAB-treated silver NC thin film sensors were measured at 303 K and 323 K from 0 V to 10 V to confirm the resistance change (Fig. 3(a)). The results confirmed that the resistance was greater at 323 K than at 303 K

and the resistance varied with temperature. Next, we measured the resistance changes in the temperature sensors at intervals of 5 K over the range from 303 K to 323 K to determine the relative resistance change (Fig. 3(b)). The relative resistance changes at 308, 313, 318, and 323 K were 0.01792, 0.03777, 0.05601, and 0.07648, respectively, confirming that the change in resistance was linear with the change in temperature. Finally, cycle tests were conducted at 303 K and 323 K to confirm the stability of the temperature sensors (Fig. 3(c)). The change in relative resistance based on variations in temperature was measured, and stable temperature-resistance properties were confirmed based on a constant resistance at each temperature.

Through the evaluation of electrothermal properties, the performance of the resistive-type temperature sensor fabricated using inkjet printing was confirmed. The TCR of the temperature sensor was $3.82 \times 10^{-3}\ K^{-1}$, and we confirmed that the resistance-type temperature sensor was successfully fabricated through the inkjet printing process.

To confirm the performance of the fabricated temperature sensors, measurements of the temperature change of a fan heater were conducted. The temperature sensor was placed in front of a fan heater equipped with heating/cooling functionality, and the change in a relative resistance was measured when activating the heating/cooling mode (Fig. 4(a)). The temperature change of the fan heater was measured using an IR detector, which measured the temperatures of the cooling and heating modes to be 20.9 °C and 130.6 °C, respectively. The temperature calculated based on the previously measured TCR ($3.82 \times 10^{-3}\ K^{-1}$) and resistance changes was 134.2 °C, confirming that the temperature can be successfully measured by the proposed sensor without significant error. Therefore, we confirmed that the development of low-cost simple temperature sensors is feasible based on the inkjet printing process.

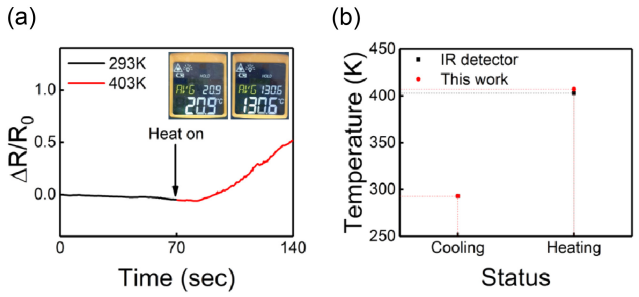

Fig. 4. Analysis using a fan heater. (a) Demo of the temperature sensor at 293 K and 403 K, (b) Comparison of measurement performances of the fabricated temperature sensors and an IR detector.

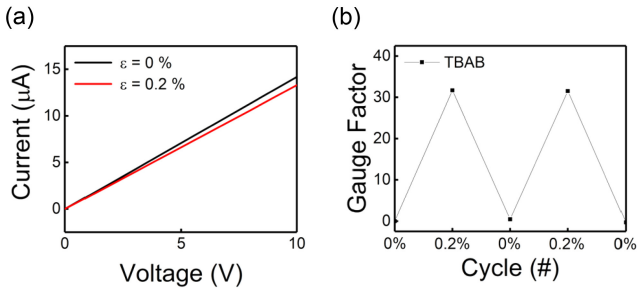

Fig. 5. TBAB-treated silver NC thin films on a 250 μm polyethylene terephthalate substrate strain sensor. (a) Electrical properties at 0% and 0.2% strain from 0 V to 10, (b) Bending test data at 0% to 0.2% strain at 10 V.

The electrical and electromechanical properties of TBAB-treated silver NC thin film strain sensors fabricated through inkjet printing were investigated. The performance of a strain sensor can be determined based on its gauge factor (GF), which is expressed as

$$GF = (\Delta R/R_0)/\varepsilon, \quad (2)$$

where ΔR, R_0, and ε are the resistance change, initial resistance, and strain, respectively.

An I-V curve was measured under the conditions of $\varepsilon = 0\%$ and 0.2% to confirm the resistance change of the strain sensors (Fig. 5(a)). The results indicate that the resistance was higher at 0.2% strain compared to that at 0% strain and that the resistance changed with the change in strain. Next, a bending test was conducted under strains of 0% and 0.2% to investigate the stability of the sensors (Fig. 5(b)). The results indicate that the resistance changed as a result of changes in strain, confirming that the sensors achieved stable electromechanical properties by showing a certain level of resistance based on the strain conditions.

These measurements of the electromechanical characteristics show that the strain sensors fabricated by inkjet printing operate normally at low strain such as at 0.2%. The GF was calculated to be 30.6, which is sufficient for use as a strain sensor. Therefore, we confirm that the fabrication of temperature and strain-detectable multi-sensors was successful through the inkjet printing process.

4. CONCLUSIONS

In this work, the surface tension and viscosity of silver nanocrystal ink were adjusted to produce uniform patterns with

one-step inkjet printing. Subsequently, a temperature and strain detectable multi-sensor was fabricated by adjusting the electrical, electrothermal, electromechanical properties using the ligand exchange process. The results of this study are expected to contribute significantly to nanocrystal-based wearable sensor fields because our proposed sensors are based on a process that is simple, low cost, and requires little time. Furthermore, these sensors can be a source technology that enables the development of future-oriented devices such as e-skin.

ACKNOWLEDGMENTS

This research was supported by the National Research Foundation of Korea grant funded by the Korea government (2020M3H4A1A02084898). This work was also supportted by National Research Foundation of Korea grant funded by the Korea government (2020M3H4A3081833). The manuscript was prepared through the contributions of all authors. All authors have given their approval for the final version of the manuscript.

REFERENCES

[1] J. Jang, H. Jung, Specification optimization and sensitivity analysis of Si_3N_4/SiO_2 slot and ridge-slot optical waveguides for integrated-optical biochemical sensors, *J. Sens. Sci. Technol.*, Vol. 30, No. 3, pp. 139-147, 2021.

[2] S. Hur, J. H. Park, S. K. Choi, C. W. Lee, and J. W. Kim, "Sensor technology for environmental monitoring of shrimp farming, *J. Sens. Sci. Technol.*, Vol. 30, No. 3, pp. 154-164, 2021.

[3] H. Joh, S. W. Lee, M. Seong, W. S. Lee, and S. J. Oh, "Engineering the charge transport of Ag nanocrystals for highly accurate, wearable temperature sensors through all-solution processes, *Small.*, Vol. 13, No. 24, p. 1700247, 2017.

[4] H. Kim, S. W. Lee, H. Joh, M. Seong, W. S. Lee, M. S. Kang, J. B. Pyo, and S. J. Oh, "Chemically Designed Metallic/Insulating Hybrid Nanostructures with Silver Nanocrystals for Highly Sensitive Wearable Pressure Sensors, *ACS Appl. Mater. & Interfaces*, Vol. 10, No. 1, pp 1389-1398, 2018.

[5] S. W. Lee, H. Joh, M. Seong, W. S. Lee, J. H. Choi, and S. J. Oh, "Transition States of Nanocrystal Thin Films During Ligand Exchange Processes for Potential Application in Wearable Sensors, *ACS Appl. Mater. & Interfaces.*, Vol. 10, No. 30, pp. 25502-25510, 2018.

[6] W. S. Lee, D. Kim, B. Park, H. Joh, H. K. Woo, U. K. Hong, T. I. Kim, D. H. Ha, and S. J. Oh, "Multi-axial and transparent strain sensors based on synergetically reinforced and orthogonally cracked hetero-nanocrystal solids, *Adv. Funct. Mater.*, Vol. 29, No. 4, p. 1806714, 2019.

[7] H. Joh, W. S. Lee, M. S. Kang, M. Seong, H. Kim, J. Bang, S. W. Lee, M. A. Hossain, and S. J. Oh, "Surface Design of Nanocrystals for High-Performance Multifunctional Sensors in Wearable and Attachable Electronics, *Chem. Mater.*, Vol. 31, No. 2, pp. 436-444, 2019.

[8] H. K. Woo, H. Kim, S. Jeon, W. S. Lee, J. Ahn, J. Bang, M. S. Kang, and S. J. Oh, "One-step chemical treatment to design ideal nanospacer structure for highly sensitive and transparent pressure sensor, *J. Mater. Chem. C.*, Vol. 7, No. 17, pp. 5059-5066, 2019.

[9] S. Jeon, J. Ahn, H. Kim, H. K. Woo, J. Bang, W. S. Lee, D. Kim, M. A. Hossain, and S. J. Oh, "Investigation of chemical effect of solvent during ligand exchange on nanocrystal thin films for wearable sensor applications, *J. Phys. Chem. C.*, Vol. 123, No. 17, pp. 11001-11010, 2019.

[10] J. Bang, W. S. Lee, B. Park, H. Joh, H. K. Woo, S. Jeon, J. Ahn, T. I. Kim, and S. J. Oh, "Highly Sensitive Temperature Sensor: Ligand-treated Ag Nanocrystal thin films on PDMS with Thermal Expansion Strategy, *Adv. Funct. Mater.*, Vol. 29, No. 32, p. 1903047, 2019.

[11] J. Ahn, S. Jeon, W. S. Lee, H. K. Woo, D. Kim, J. Bang, and S. J. Oh, "Chemical Effect of Halide Ligands on the Electromechanical Properties of Ag Nanocrystal Thin Films for Wearable Sensors, *J. Phys. Chem. C.*, Vol. 123, No. 29, pp. 18087-18094, 2019.

[12] B. K. Jung, S. Jeon, H. K. Woo, T. Park, J. Ahn, J. Bang, S. Y. Lee, Y. M. Lee, and S. J. Oh, "Janus-like Jagged Structure with Nanocrystals for Self-sorting Wearable Tactile Sensor", *ACS Appl. Mater. & Interfaces.*, Vol. 13, No. 5, pp. 6394-6403, 2021.

[13] T. Park, H. K. Woo, B. K. Jung, B. Park, J. Bang, W. Kim, S. Jeon, J. Ahn, Y. Lee, Y. M. Lee, T. I. Kim, and S. J. Oh, "Non-Interference Wearable Strain Sensor: Near-Zero Temperature Coefficient of Resistance Nanoparticle Arrays with Thermal Expansion and Transport Engineering", *ACS Nano.*, Vol. 15, No. 5, pp. 8120-8129, 2021.

[14] C. R. Kagan, and C. B. Murray, "Charge transport in strongly coupled quantum dot solids", *Nat. Nanotechnol.,* Vol. 10, No. 12, pp. 1013-1026, 2015.

[15] J. H. Choi, A. T. Fafarman, S. J. Oh, D. K. Ko, D. K. Kim, B. T. Diroll, S. Muramoto, J. G. Gillen, C. B. Murray, and C. R. Kagan, "Bandlike transport in strongly coupled and doped quantum dot solids: a route to high-performance thin-film electronics", *Nano Lett*., Vol. 12, No. 5, pp. 2631-2638, 2012.

[16] R. C. Doty, H. Yu, C. K. Shih, and B. A. Korgel, Temperature-dependent electron transport through silver nanocrystal superlattices, *J. Phys. Chem. B.,* Vol. 105, No. 35, pp. 8291-8296, 2001.